# Spring tropical cyclones modulate near-surface isotopic compositions of atmospheric water vapour at Kathmandu, Nepal

Niranjan Adhikari[1, 2], Jing Gao[1, 3,*], Aibin Zhao[1], Tianli Xu[1, 4] Manli Chen[1, 3], Xiaowei Niu[1], Tandong Yao[1, 3]

[1] *State Key Laboratory of Tibetan Plateau Earth System, Resources and Environment, Institute of Tibetan Plateau Research, Chinese Academy of Sciences, Beijing 100101, China*

[2] *University of Chinese Academy of Sciences, Beijing 100049, China*

[3] *Lanzhou University, Lanzhou 733000, China*

[4]*Kathmandu Centre for Research and Education,* Chinese Academy of Sciences *–Tribhuvan University, Kirtipur 44613, Kathmandu, Nepal*

* Correspondence to: Jing Gao, E-mail: gaojing@itpcas.ac.cn

## S1 Humidity isotope response calibration

Determining isotopic composition with an analyser based on cavity ring-down spectroscopy (CRDS) can introduce an artificial isotopic signal depending on the humidity of the introduced air samples unless the instruments are properly calibrated for humidity (Steen-Larsen et al., 2013). Even for unknown samples, this effect can be corrected if the correction function is determined using vapour with a known isotopic composition. When conducting our humidity-isotope response calibration, we introduced both standard samples at different humidity levels that covered the full range of atmospheric humidity. The instrument exhibits a transient response when switching between humidity levels. Thus, to obtain a reliable humidity-isotope transfer function the duration of this transient response must be excluded from the actual measurement. For this, the flow rate of dry air was kept constant for 25 min at each humidity level and then changed gradually. To overcome any memory effect, we excluded the first 15 minutes of data acquisition from the calculations of the humidity-isotope response function. We also excluded data if the humidity appeared unstable. To remove analyser drift, we chose a reference humidity level from within typical atmospheric humidity ranges. As mentioned earlier, we performed daily measurements of each standard sample at three water vapour concentration levels, using a humidity value of close to 20,000 ppmv as a constant reference humidity level. The raw data were converted to humidity-corrected values by applying the resulting humidity-isotope response functions (Fig. S1).

Raw data collected between 7 May and 15 May 2021 was calibrated using the humidity-isotope response function obtained on 18 April 2021, and data collected from 15 May onwards was calibrated using the humidity-isotope response function obtained on 15 May 2021.
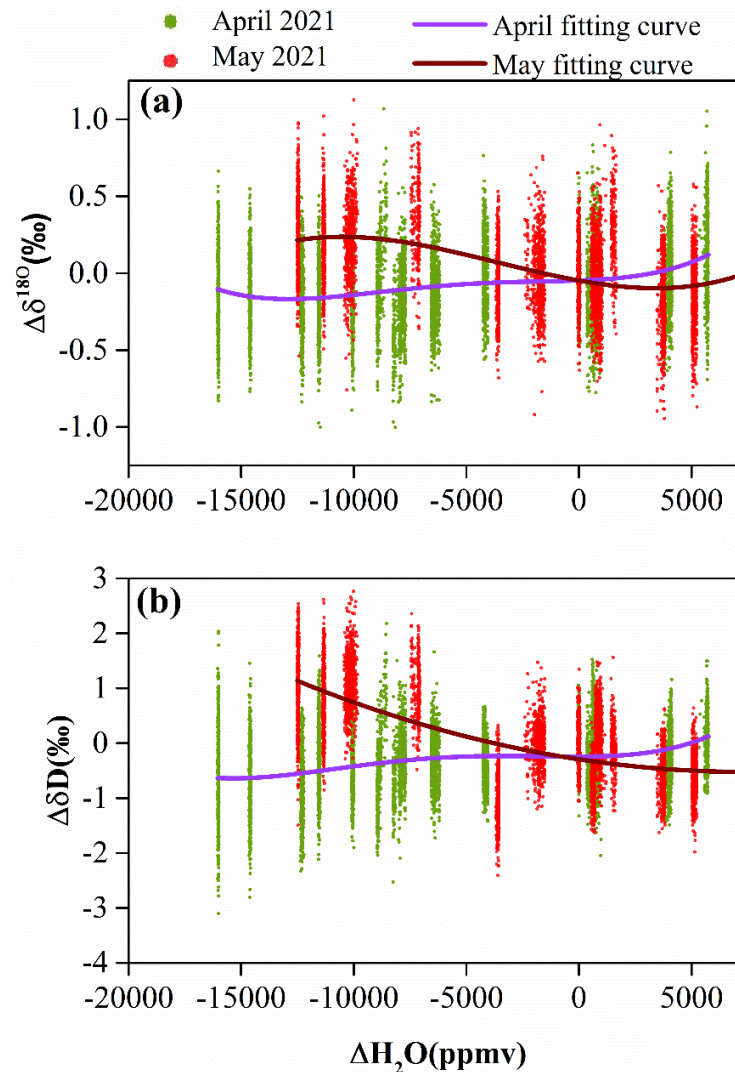
**Figure S1 Humidity-isotope response functions of the Picarro analyser for (a) $\delta^{18}O$ and (b) $\delta D$. The y-axis shows the bias with respect to the mean value measured at the reference humidity level (~20,000 ppmv).**

## S2 Known standard calibration

To correct instrument bias of measured $\delta^{18}O$ and $\delta D$ values, we used two standards of known isotopic compositions (S1: $\delta^{18}O$ = -29.674 ‰ and $\delta D$ = -225.827 ‰ and S2: $\delta^{18}O$ = -10.081 ‰

and δD = -69.122 ‰) to computed a transfer function and convert the measurement to the international VSMOW scale. Each standard was injected for 25 minutes at three different humidity levels to minimize the memory effect, averaging over the last 15 minutes to obtain the transfer function by applying two-point normalization to the standard and averaged values. The function was assumed to be linear, of the form y=mx+c. We computed the transfer function for each day to convert the humidity-corrected values of $\delta^{18}O$ and δD to VSMOW scale.

Figure S2 shows the data used for the calibration and resulting VSMOW slopes ranging from 0.98 to 1.01 for δD and from 0.99 to 1.03 for $\delta^{18}O$.
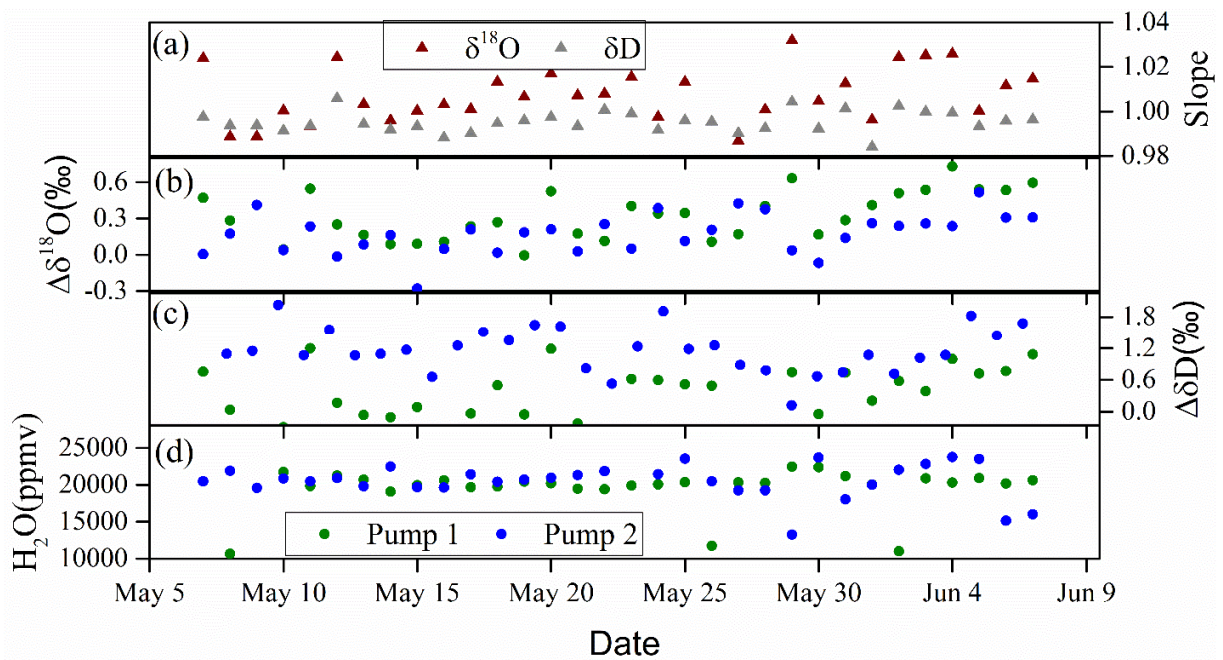
**Figure S2 Picarro measurements of known standard samples used for calibration. (a) VSMOW slopes, (b,c) difference between true and measured isotopes ($\delta^{18}O$ and δD) values of standard samples, and (d) reference humidity levels.**
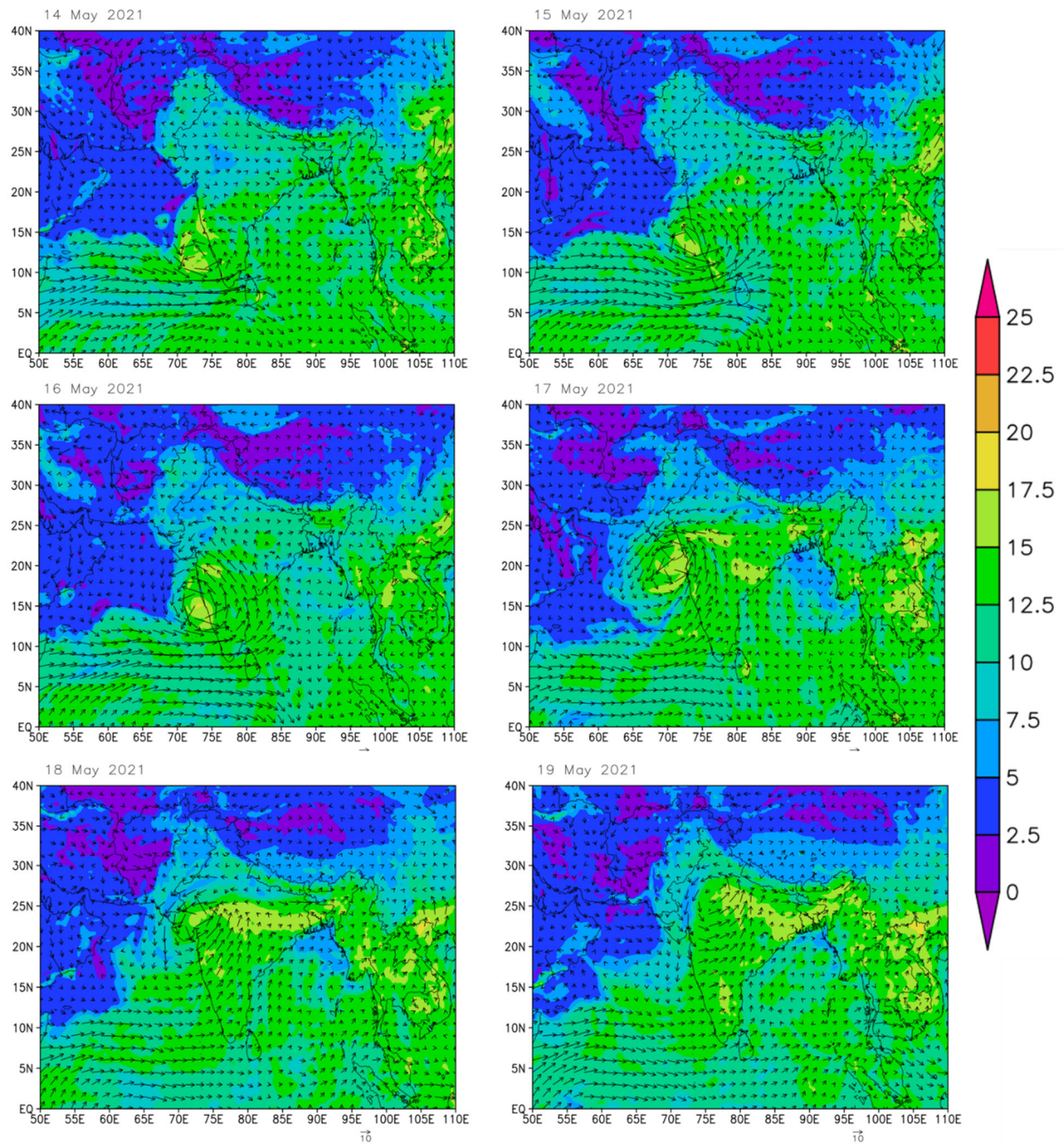
**Figure S3 Regional wind distribution pattern (arrows) and specific humidity (colours, g/kg) during cyclone Tauktae, showing its formation over the Arabian Sea and northward trajectory.**
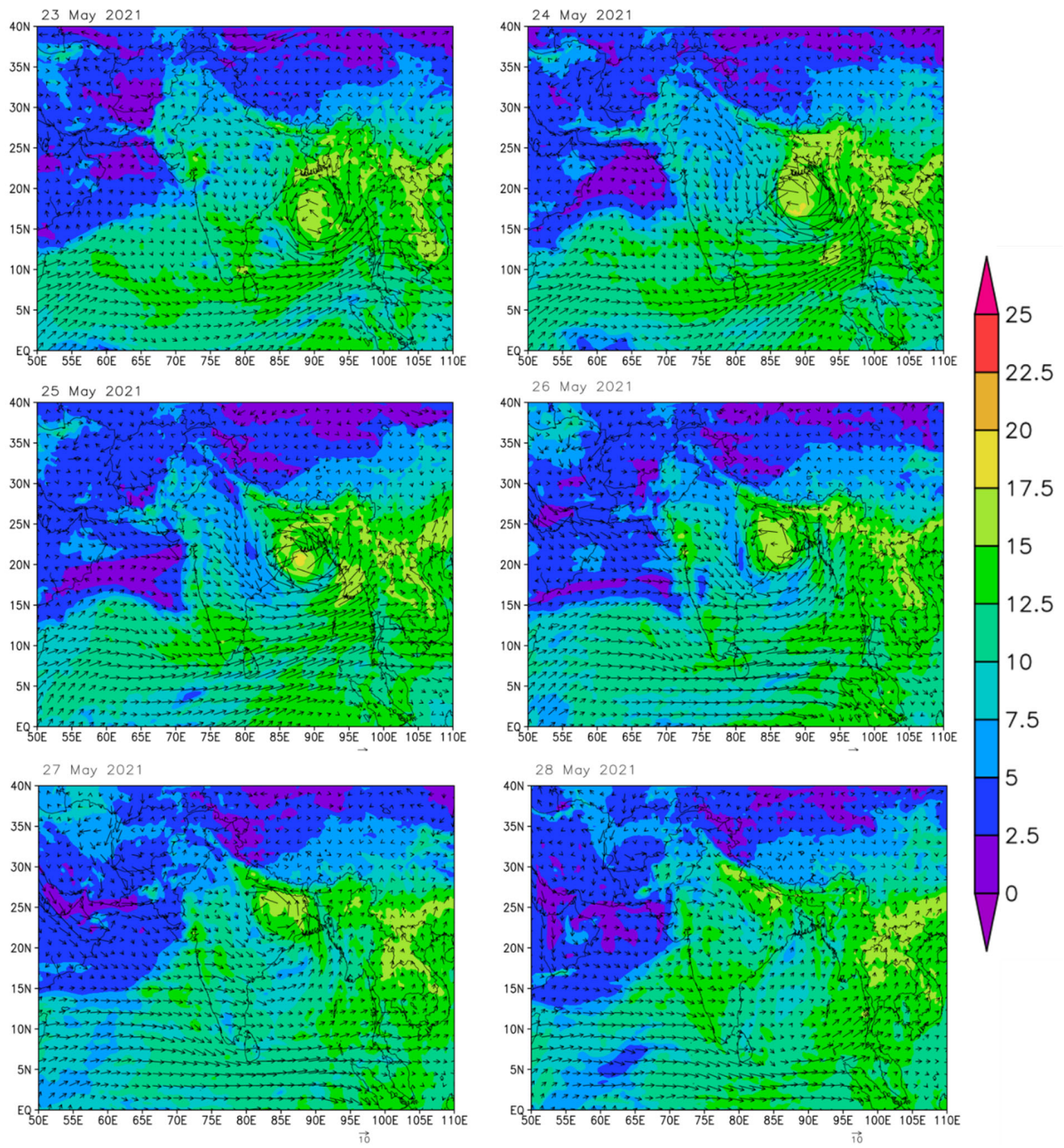
**Figure S4 As in Figure S3 but for cyclone Yaas that formed over the Bay of Bengal.**
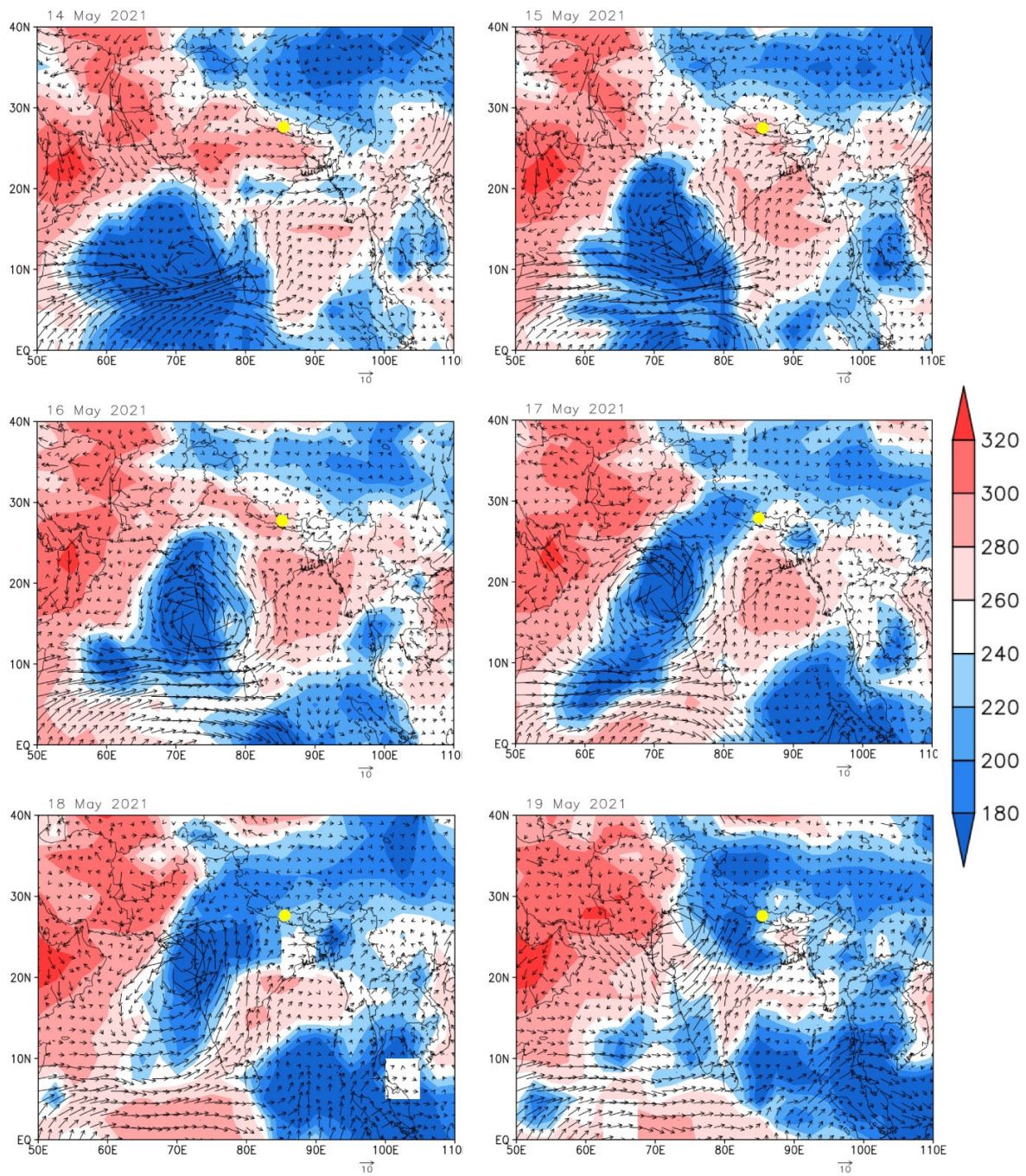
**Figure S5 Regional winds (arrows) and outgoing longwave radiation (colours in Wm$^{-2}$) during cyclone Tauktae.**
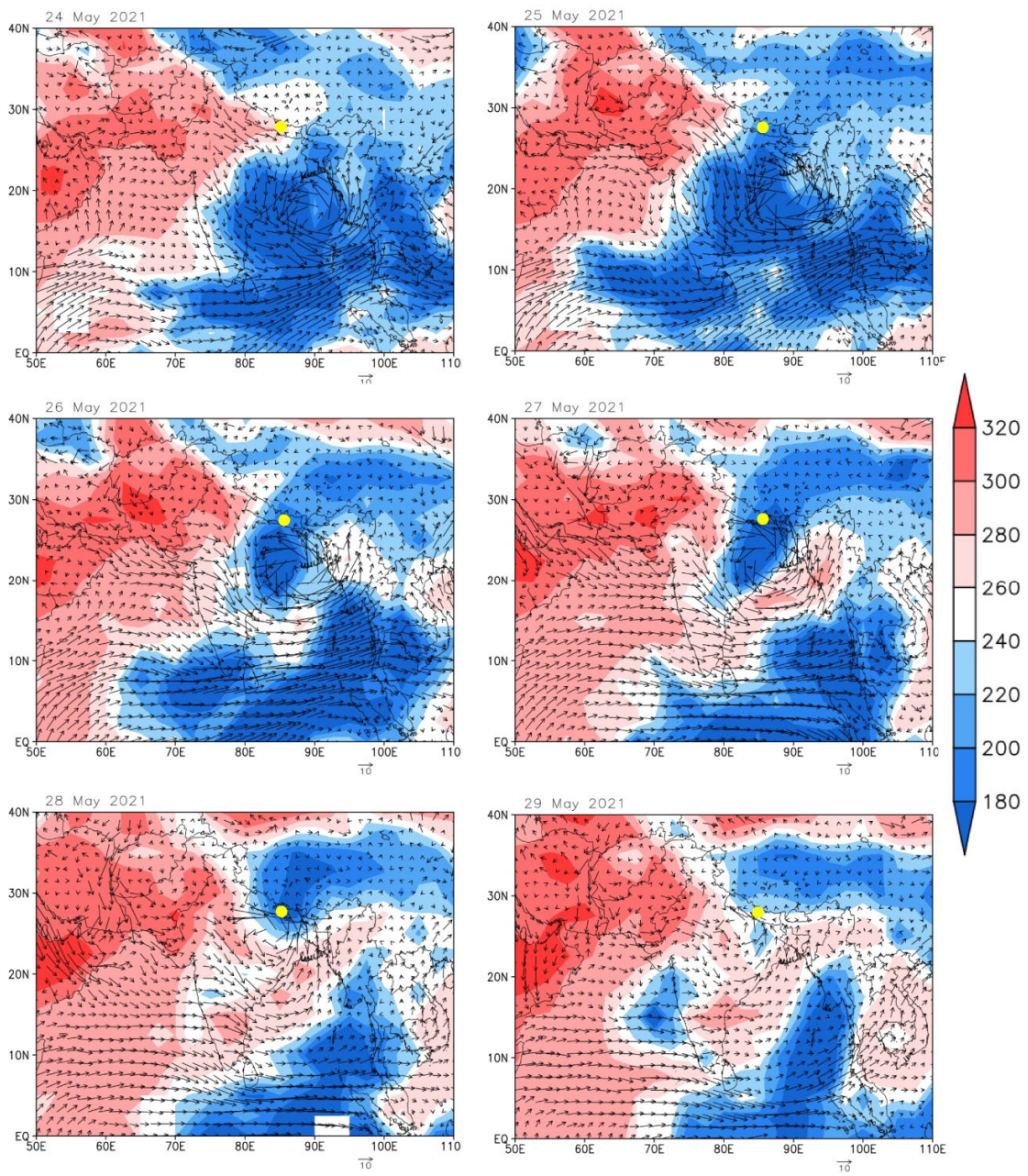
**Figure S6 As in Figure S5 but for cyclone Yaas.**
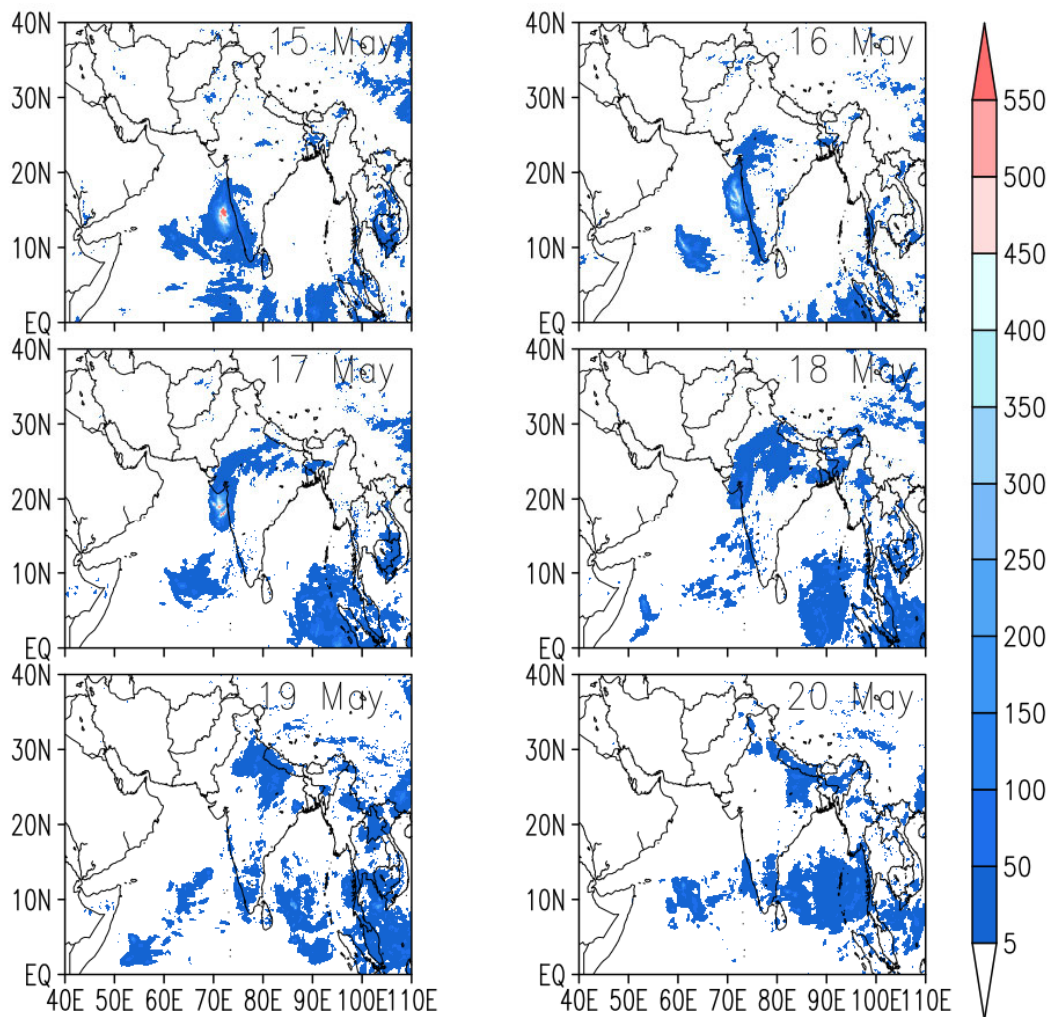
**Figure S7 Regional precipitation in millimeters (mm) retrieved from the Integrated Multi-satellite Retrievals for GPM (IMERG) from the Global Precipitation Measurement (GPM) programme during cyclone Tauktae.**
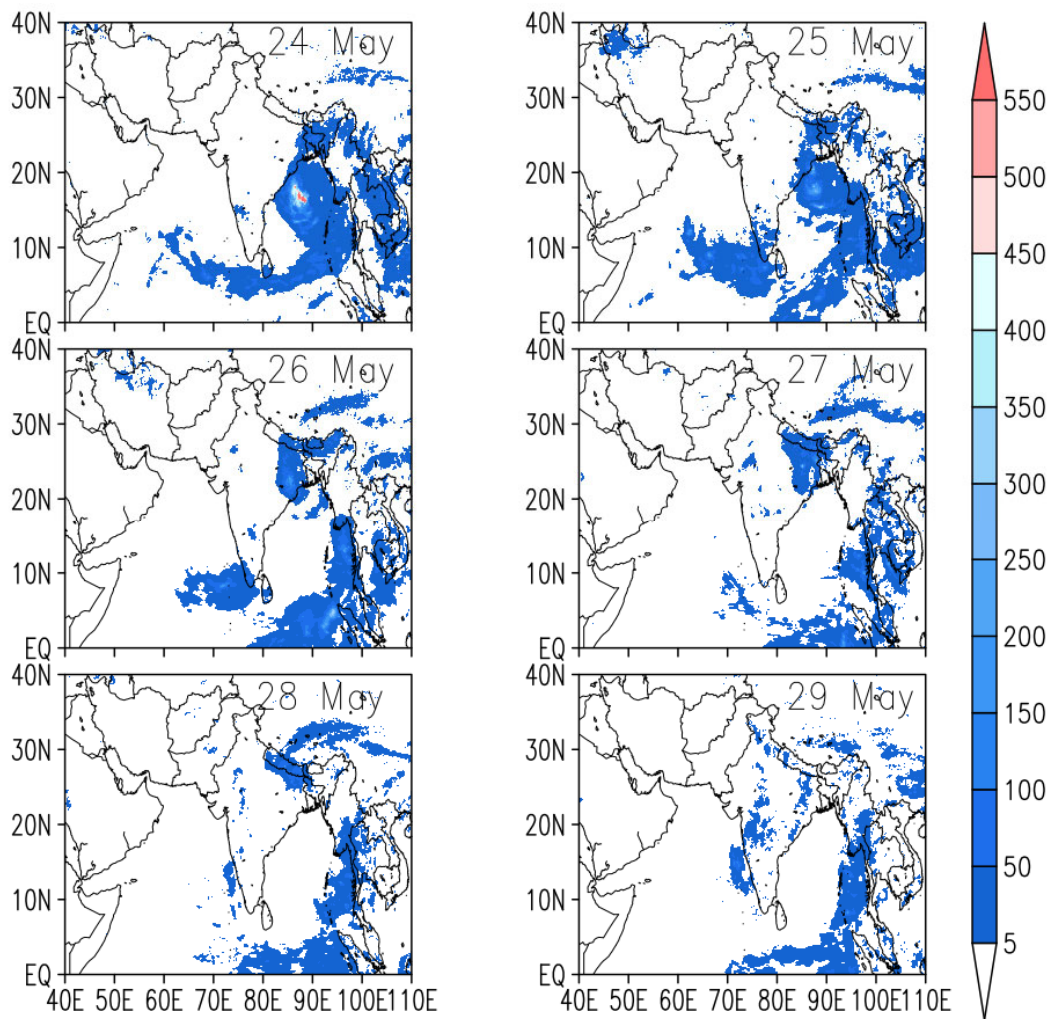
**Figure S8 As in Figure S7 but for cyclone Yaas.**
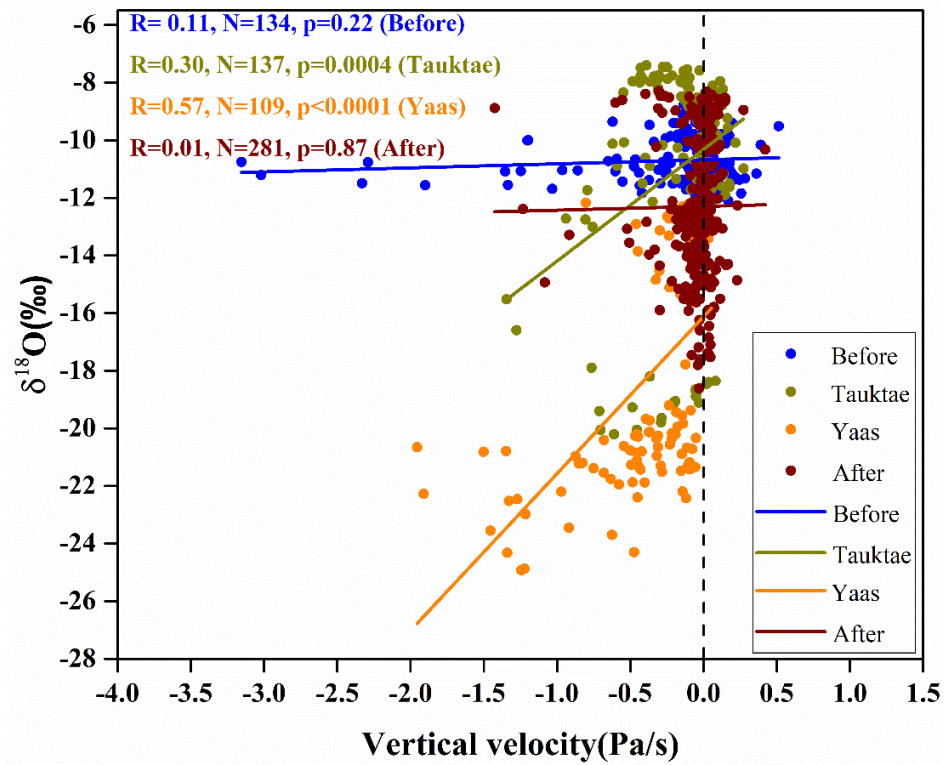
**Figure S9 Linear regression between $\delta^{18}O_v$ and the average vertical velocities at pressure levels between 300 hPa and 600 hPa, averaged over 25° N-28° N and 83° E-87° E which has our measurement site near its centre. The vertical black dashed line represents the threshold separating ascending (negative values) and descending (positive values) air motions.**
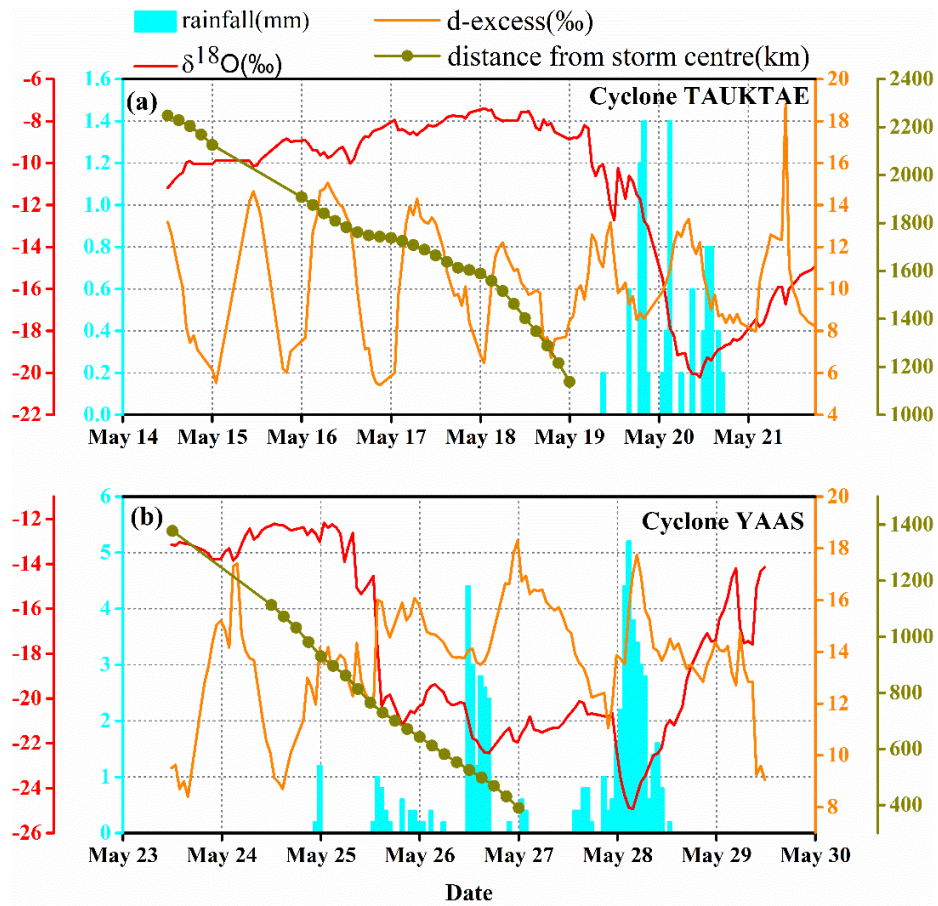
**Figure S10 Observed isotopic contents, distance between cyclone eye and sampling site, and related rainfall amount during cyclones Tauktae (a) and Yaas (b).**